BROOKHAVEN NATIONAL LABORATORY

BNL-94638-2011

Susceptibility of Granite Rock to $scCO_2$/Water at 200°C and 250°C

**Toshifumi Sugama, Simerjeet Gill, Lynne Ecker,
Thomas Butcher, and John Warren**

January 2011

Sustainable Energy Technologies Department

Brookhaven National Laboratory

**U.S. Department of Energy
DOE Energy Efficiency and Renewable Energy
DOE Geothermal Technologies Program**

DISCLAIMER

Susceptibility of Granite Rock to scCO_2/Water at 200°C and 250°C

Toshifumi Sugama, Simerjeet Gill, Lynne Ecker, Thomas Butcher,
and John Warren
Brookhaven National Laboratory

Daniel Bour
AltaRock Energy, Inc.

January 2011

U.S. Department of Energy
[DOE Energy Efficiency and Renewable Energy],
[DOE Geothermal Technologies Program]

Susceptibility of Granite Rock to scCO_2/Water at 200°C and 250°C

Prepared for

The U.S. Department of Energy
Energy Efficiency and Renewable Energy
Geothermal Technologies Program
1000 Independence Avenue SW
Washington, D.C. 20585

Prepared by

Toshifumi Sugama, Simerjeet Gill, Lynne Ecker, Thomas Butcher,
and John Warren

Brookhaven National Laboratory
Upton, NY 11973-500

Daniel Bour
AltaRock Energy, Inc.

January 2011

Abstract

Granite rock comprising anorthoclase-type albite and quartz as its major phases and biotite mica as the minor one was exposed to supercritical carbon dioxide ($scCO_2$)/water at 250°C and 13.78 MPa pressure for 104 hours. For comparison purpose, four other rocks, albite, hornblende, diorite, and quartz, also were exposed. During the exposure of granite, ionic carbonic acid, known as the wet carbonation reactant, preferentially reacted with anorthoclase-type albite and biotite, rather than with quartz. The susceptibility of biotite to wet carbonation was higher than that of anorthoclase-type albite. All the carbonation by-products of anorthoclase-type albite were amorphous phases including Na- and K-carbonates, a kaolinite clay-like compound, and silicon dioxide, while wet carbonation converted biotite into potassium aluminum silicate, siderite, and magnesite in crystalline phases and hydrogen fluoride (HF). Three of these reaction by-products, Na- and K-carbonates and HF, were highly soluble in water. Correspondingly, the carbonated top surface layer, about 1.27 mm thick as carbonation depth, developed porous microstructure with numerous large voids, some of which have a size of ≥ 10 μm, reflecting the erosion of granite by the leaching of these water-soluble reaction by-products. Comparing with this carbonation depth, its depth of other minerals was considerable lower, particularly, for hornblende and diorite with 0.07 and 0.02 mm, while no carbonate compound was detected in quartz. The major factor governing these low carbonation depths in these rocks was the formation of water-insensitive scale-like carbonate by-products such as calcite ($CaCO_3$), siderite ($FeCO_3$), and magnesite ($MgCO_3$). Their formation within the superficial layer of these minerals served as protective barrier layer that inhibits and retards further carbonation of fresh underlying minerals, even if the exposure time was extended. Thus, the coverage by this barrier layer of the non-carbonated surfaces of the underlying rock was reason why the hornblende and diorite exhibited a minimum depth of carbonation. Under exposure to the $scCO_2$/water at 200°C and 10.34 MPa pressure for up to 42 days, the ranking of the magnitude of erosion caused by wet carbonation was in the following order; granite > albite > hornblende > diorite > quartz. The eroding-caused weight loss of granite (0.88 %) was ~2.4, ~5.2, ~9.8, and ~17.6 times greater than that of albite, hornblends, diorite, and quartz, respectively.

Introduction

Supercritical carbon dioxide ($scCO_2$) has attractive properties as an alternative working fluid in the enhanced geothermal system (EGS) because of its excellent convective heat transportation properties associated with its high thermal conductivity, volume expansion nature, low surface tension, and low viscosity as well as its high flow rate relative to its low density, compared with that of water [1-4]. However, one inevitable issue about the use of $scCO_2$ is its reactivity with EGS's reservoir rock minerals at temperatures of ≥ 200°C, particularly, in the moisture-containing environment. The chemical affinity of $scCO_2$/water with rock minerals, known as wet carbonation, may engender in them the undesirable carbonation reaction by-products, which are vulnerable to water, raising concerns that the solubility of reaction by-products in water may impair the integrity of the reservoir rock's structure. Thus, it is very important to know about what kinds of reaction by-products are formed by the wet carbonation of the rock minerals present in the EGS well sites within an impermeable, hard, dense stratum.

Our previous study [5] focused on three objectives: First, to identify the carbonation by-products of representative rock minerals in the EGS sites; second, to clarify the carbonation reaction mechanisms for each mineral; third, to rank and classify the magnitude of susceptibility of various different rock minerals to wet carbonation based upon the results obtained from first and second objectives. To meet these objectives, we exposed powdered pure mineral pastes made with water for 3 days to $scCO_2$/water at 250°C and 2500 psi (17.23 MPa) pressure. Among the pure rock minerals used in this study were granite, albite, biotite, hornblende, and diorite. The carbonation of the first two minerals yielded alkali metal Na- and K-carbonates coexisting with two other by-products, kaolinite clay-like aluminum silicate hydroxide and amorphous silica. In contrast, the carbonation of biotite, hornblende, and diorite generated Ca-, Mg-, and Fe-carbonates. In rationalizing the rock mineral's susceptibility to wet carbonation based upon the feldspar ternary diagram, we concluded that its susceptibility of various different minerals in the plagioclase feldspar family depended primarily on the amount of anorthite phase. Correspondingly, the alkali feldspar minerals involving anorthoclase-

type albite and sanidine had a lower reactivity with $scCO_2$, compared with that of plagioclase feldspar minerals.

Regarding the other carbonation by-products, our consideration attention was paid to the physicochemical behaviors of aluminum silicate hydroxide-based clay-like by-products because some clay minerals display undesirable large water uptake, disintegration, and excessive volume expansion that might generate in-situ stress in a critical boundary zone between clay and non-clay mineral layers. The chemistry of the clay-like by-products derived from these rock minerals was similar to that of kaolinite clay, $Al_2Si_2O_5(OH)_4$. Although clay minerals constituted only a minor portion of the dense impervious rock stratum in EGSs, we explored the wet carbonation of three clay minerals, bentonite, kaolinite, and soft-clay, after exposure them for 72 and 107 hours to $scCO_2$/water at 200° and 250°C [6]. Among these clay minerals, the bentonite was most susceptible to wet carbonation, leading to its disintegration and fragmentation during the exposure. Its fragmentation was due to the dissolution of by-products formed by the carbonation of montomorillonite (MMT) and anorthoclase-type albite phases present in bentonite. In contrast, kaolinite and soft-clay were chemically inert to wet carbonation, except for weight gain due to their water uptake. This fact strongly suggested that kaolinite-like by-products yielded by the wet carbonation of rock minerals might remain unchanged, even through extended exposure.

Throughout the world, the commonest rock facing EGS's drilling operators is dense, hard granite with its minimum water permeability [7]. Our previous study discussed above, on its carbonation was made on powdered samples, but not balk rock. Therefore, our emphasis in this present study was directed towards evaluating alteration of bulk granite rock after exposure to $scCO_2$/water at 250°C. The factors to be evaluated included the profile of its wet carbonation depth, the morphological alteration of microstructure developed by its wet carbonation, and the hypothesis why such a microstructure forms. Additionally, we monitored the change in its weight as a function of exposure time for up to 42 days at 200°C. To support these data, we reviewed the findings from the powdered samples on the chemistry of carbonated and non-carbonated granite.

For comparison, the other bulk rock minerals, such as albite, hornblende, diorite, and quartz, also were exposed to $scCO_2$/water at 200° and 250°C, and then we measured their carbonation depths and monitored their weight changes. Integrating all information described above gave us insights about the effect of the wet carbonation on granite and whether it is vulnerable to hot wet carbonation at ≥ 200°C.

Experimental

Five rock minerals, granite, albite, hornblende, diorite, and quartz, were obtained from Rockman's Trading Post, Inc. For only granite, the powdered sample was used to review the phase identification, the carbonation-induced reaction products, and the mechanisms of carbonation. We prepared the sample in the following manners: The granite was broken down and grounded into particle size of < 0.2 mm. The powder then was mixed with a water to prepare mineral paste; the ratio of water/powdered granite by weight was 19.1 %. Then, the past was inserted into 1-cm diameter x 5-cm long quartz vials; the thickness of the past adhering to vial wall's surface was approximately 3 mm. The vial was exposed for 72 hours in an autoclave containing $scCO_2$ at 250°C under the helium pressure of 2500 psi (17.23 MPa).

The unadulterated these five bulk rocks were used to obtain information on carbonation depth-profiling and changes in weight caused by wet carbonation. For the carbonation profiling study, the $scCO_2$ exposure test of these rocks was conducted according to the following sequences: 1) The rocks were placed in autoclave containing water (~ 5 % of autoclave's volume), 2) the temperature in autoclave was raised to 120°C to generate steam, 3) $scCO_2$ was fed into the steam at pressure of 2000 psi (13.78 MPa), and 4) autoclave temperature then was increased to 250°C for 104 hours. Using the same exposure test procedure as that described above, except for three different parameters; the autoclave temperature at 200°C, pressure of 1500 psi (10.34 MPa), and the exposure time of 42 days, we monitored the changes in weight of these rock samples as a function of exposure time.

Thereafter, all powdered and rock samples were dried in an oven at 100°C for 24 hours to eliminate all moisture adsorbed and penetrated in the samples. For the exposed rock samples, we determined the carbonation depth using Optical microscopy in conjunction with Fourier transform infrared (FT-IR, model Spectrum One by Perkin Elmer Corp). X-ray powder diffraction (XRD, model XRG 3000 by Philips Electronics Corp.) and FT-IR were employed to identify crystalline and amorphous carbonation or non-carbonation products, and to estimate the extent of the susceptibility of mineralogical phases present in granite to reaction with $scCO_2$/water. The high resolution scanning electron microscopy (HR-SEM, model JEOL 7600F) concomitant with energy-dispersive X-ray (EDX) was used to detail the microstructure of granite developed by wet carbonation, and to obtain the elemental distribution of this altered microstructure.

Results and Discussion

Wet Carbonation of Granite

Figure 1 shows the different features of the x-ray diffraction patterns of granite before and after exposure to $scCO_2$. Unexposed granite contains three phases, an anorthoclase-type albite [$(Na,K)AlSi_3O_8$] belonging to the family of alkali feldspar, biotite mica [$K(Fe,Mg)_3AlSi_3O_{10}(F,OH)_2$] and quartz (SiO_2). When the granite was exposed, the feature of diffraction pattern differed from that of the unexposed one. There were two major differences: One was the decay of the intensity of all anorthoclase-type albite- and biotite-related XRD lines, while the line intensity of quartz-associated d-spacing remained unchanged; the other was the formation of three new crystalline products, potassium aluminum silicate ($KAlSiO_4$), siderite ($FeCO_3$), and magnesite ($MgCO_3$), due to the wet carbonation of biotite. To verify that biotite's wet carbonation led to the formation of these carbonation products, the pure powder biotite past (water/powder ratio= 63.8 wt%) was exposed under the same $scCO_2$ condition as that of granite. As evident in Figure 2, the XRD analytical results strongly supported the fact that the exposure of biotite phase in granite converted it into these three crystalline carbonation reaction products. In addition, this result revealed that the wet carbonation of biotite generated quartz. Relating this XRD pattern's feature to that of exposed granite (figure

1), some *d*-spacing lines attributed to these reaction products appeared to overlap anorthoclase-type albite-related spacing lines.

Returning to figure 1, to reveal which phase, anorthoclase-type albite or biotite, is more susceptible to carbonation, we inspected the area ratios between the representative *d*-spacing peaks for the anorthoclase-type albite-, biotite-, and quartz-phase before and after exposure (Table 1). For unexposed granite, the peak area ratios of anorthoclase-type alibite (Aa), d_{002}/ quartz (Q), d_{101}, biotite (B), d_{001}/ quartz (Q), d_{101}, and biotite (B), d_{001}/ anorthoclase-type alibite (Aa), d_{002} were 0.80, 0.25, and 0.31, respectively, demonstrating that both the anorthoclase-type albite and quartz are present as the major phases in granite; biotite can be described as the minor phase. After exposure, the Aa, d_{002}/ Q, d_{101} ratio declined by 39 % to 0.49, compared with that of unexposed rock. In contrast, the B, d_{001}/ Q, d_{101} ratio of 0.09 corresponded to a drop of 64 % from that of unexposed one. Hence, the reactivity of biotite with $scCO_2$/water was notably higher than that of anorthoclase-type albite.

Figure 3 gives the FT-IR spectra for granite before and after exposure. A typical spectrum from unexposed granite had the following absorption bands: At 2438 cm^{-1} ascribed to O-H stretching vibration in H_2O, adsorbed to quartz; at 1978 and 1870 cm^{-1}, originating from the Si-O stretching mode in quartz [8], at 1611 cm^{-1} due to adsorbed H_2O; at 1097 and 998 cm^{-1}, corresponding to the oxygen-bridging Si-O-Si asymmetric stretching and non oxygen-bridging $Si-O^-$ stretching [9,10] in anorthoclase-type albite and biotite; and at the range from 776 to 725 cm^{-1} assigned to Al-O stretching [11] in anorthoclase-type albite and biotite.

For exposed samples, the attention was paid to the appearance of two new absorption bands at 1568 and 1420 cm^{-1}, and the shift of non oxygen-bridging $Si-O^-$ band to lower wavenumber site, from 998 to 923 cm^{-1}. Since the oxygen in this last band is linked directly to Na^+ and K^+ cations, this sift to the SiOH-related band site suggests that $scCO_2$ ruptured the linkage between SiO^- and Na^+ or K^+. Hence, there is no reason to doubt that the band at 1420 cm^{-1} reflected the amorphous sodium- and potassium-carbonates,

Na_2CO_3 and K_2CO_3 [12], in anorthoclase-type albite. It should be noted the band at 1420 cm^{-1} also includes CO_3^{2-} in the siderite- and magnesite-crystals yielded by the carbonation of biotite.

As is well documented [13,14], the reactions between CO_2 and water lead to the generation of ionic carbonic acid, $CO_2 + H_2O \leftrightarrow HCO_3^- + H^+ \leftrightarrow CO_3^{2-} + 2H^+$. These carbonates might be formed through the following wet carbonation reaction of anorthoclase-type albite in granite, $2(Na,K)AlSi_3O_8 + 2CO_3^- + 4H^+ \rightarrow Na_2CO_3 + K_2CO_3 + Al_2Si_{6-x}O_{12-2x}(OH)_4 + xSiO_2$. Some silicon dioxide may be precipitated as reaction by-products [15]. If so, the band at 1568 cm^{-1} could be associated with the formation of the kaolinite clay-like mineral, $Al_2Si_{6-x}O_{12-2x}(OH)_4$, containing SiOH groups as the amorphous carbonation by-product. On the other hand, the carbonation reaction of biotite might be represented as follows, $K(Fe,Mg)_3AlSi_3O_{10}(F,OH)_2 + 6CO_3^{2-} + 12H^+ \rightarrow KAlSiO_4 + 2SiO_2 + 3MgCO_3 + 3FeCO_3 + 2HF + 2OH^- + 10H^+$. In this reaction, all reaction products, except for HF and other ionic species, were crystalline compounds; in contrast, all anorthoclase-type albite's carbonation reaction products were amorphous phases. Nevertheless, we paid attention to the solubility of the carbonation products from anorthoclase-type albite and biotite in aqueous medium. The solubility of Na- and K-carbonates from anorthoclase-type albite in water is more than 10^3 times higher than that of Mg- and Fe-carbonates from biotite [16], while HF yielded by the carbonation of biotie is leached out, raising concerns about the erosion of granite.

As described in our previous report [6], the chemical affinity of such kaolinite clay-like by-products with the ionic carbonic acid was minimal, if any. Therefore, this clay-like by-product might remain well unchanged although the exposure time was extended further.

Microstructure Development of Carbonated Granite

Based upon the carbonation chemistry of granite, our study now was shifted to exploring the carbonation-depth profile, visualizing the morphology of microstructure developed in

the granite, and identifying the elemental composition of altered microstructure after exposure for 104 hours to $scCO_2$/water at 250°C and 13.78 MPa pressure.

Figure 4 shows the image from the optical microprobe of the fractured surface of exposed granite in conjunction with the FT-IR tracing of carbonation products. This image revealed the presence of two different layers: One that was darkly colored, marked as "2" appeared at the location between the top surface and ~ 1269 μm depth; the other was lightly colored beneath this depth. In addition, the adjacent area about 180 μm thick, denoted as "1", was dark green, and represented the interfacial region. We assumed that the region with a dark color was due to the carbonation of granite. To validate this assumption, we collected the samples at the loci marked as "a", "b", "c", "d", and "e" for FT-IR analysis. As described in the earlier FT-IR study, the band at 1420 cm^{-1} was assigned to CO_3^{2-} in the carbonated compounds. Thus, our focus centered on tracing this band in samples taken from these five loci. Sample "a" collected from the core region did not show any sign of this band, meaning it was a non-carbonation region. The top surface region "b" of ~ 360 μm thick had an intense band at 1420 cm^{-1}, verifying that this area encompassed carbonated products. The tendency of this band's intensity to decline can be seen as the location of the collected sample shifted toward the nearby light-colored region. In fact, the location "e" in a critical boundary zone between the dark and light regions displayed a very weak band at 1420 cm^{-1}, reflecting a minimum rate of carbonation. Additionally, this information strongly suggested that both the optical microprobe and FT-IR tracing as analytical methods have a high potential for profiling carbonation depth in granite rock. Nonetheless, the carbonation depth of granite was ~ 1269 μm after exposure of 104 hours at 250°C.

Figure 5 shows the SEM image involving three distinctive regions expressed as non-carbonated, carbonated interfacial, and well-carbonated areas, of the fractured surface. The morphological feature of the non-carbonated region was characterized by disclosing a smooth surface texture. In contrast, the carbonated interfacial region had a rough surface containing a copious pore with ≤ ~ 5 μm size. A further rough surface including large voids and cavities of ≥ ~ 10 μm size were observed in the well-carbonated region.

This finding provided us with strong evidence that the porous microstructure resulted from wet carbonation of granite.

To better understand the factors governing the creation of porous microstructure, we explored the composition of elements in these three regions by EDX coupled with SEM (Figure 6). Since the penetration depth of X-ray from EDX is ~ 1.5 μm, the resulting EDX spectra indicates the elemental composition existing in the top surface layer up to ~ 1.5 μm thick. The EDX spectrum for the non-carbonated region denoted as "A" location exhibited two dominant elemental peaks of O and Al, three moderate peaks of C, Ni, and Al, and the weak Na and K elements. These elements except for Ni are assignable to the anorthoclase-type albite and quartz. There were no signals from Mg, Fe, and F elements attributed to the biotite. The Ni seems to be present in granite as the additional element. Comparing with this spectral feature, the EDX spectrum from the carbonated interfacial region as site "B" expressed two notable differences: One is a growth of intensification of C-related signal; the other was to emerge the F element, while the other elements, such as O, Ni, Na, Al, Si, and K, still were detected. Since C and F elements are assignable to the carbonated compounds and biotite, respectively, the porous, rough interfacial region appears to contain the Na- and K-carbonates yielded from carbonated anorthoclase-type albite and the F-related by-product from carbonated biotite. As described earlier, HF might be formed through the wet carbonation of biotite. Hence, a possible interpretation is that the detected F is related to HF leached out from biotite. Further pronounced growth of the C- and F-related signal intensity along with a striking decay of O and Si signals and an elimination of Ni signal was observed in the well-carbonated region containing numerous large cavities denoted as site "C". Meanwhile, Na and K elements still exist in the top surface layer with ~ 1.5 μm thick. This fact suggested that the creation of large voids and the development of porous microstructure in the carbonated regions were due primarily to the erosion of granite brought about by the dissolution of Na- and K-carbonates and HF in the aqueous medium. During this dissolution process, these water-soluble species migrated to the outermost surface site, where they covered the water-insoluble and minimally soluble carbonation by-products, such as the clay-like compounds, quartz, potassium aluminum silicate, and Mg- and Fe-carbonates. This is the

reason why the peak intensity of O and Si was strikingly reduced, and the Ni signal eliminated in the well-carbonated region. Thus, the susceptibility of anorthoclase-type albite and biotito to wet carbonation reactions, followed by the dissolution of carbonation by-products, played an essential role in creating the rough, porous microstructure in granite, thereby entailing its erosion.

Carbonation Depth of Various Different Rocks

Figure 7 compares the carbonation depths of granite and the other rock minerals, except for quartz, determined by FT-IR depth tracing technique as detected by the CO_3^{2-} -related band at 1420 cm^{-1}. Granite had the highest rate of carbonation, corresponding to a 1.27mm depth of carbonation. The second most susceptible was albite ($NaAlSi_3O_8$), with a carbonation depth with 0.19 mm. As described in our previous report [5], we proposed the wet carbonation of albite as follows; $2NaAlSi_3O_8 + CO_3^{2-} + 2H^+ \rightarrow Na_2CO_3 + Al_2Si_6O_{14}(OH)_2$. Since the resulting Na-carbonate yielded is high soluble in water, albite also underwent some erosion due to the leaching of this carbonate. In contrast, the other two minerals, hornblende and diorite, exhibited a considerably low rate of carbonation, leading to only 0.07 and 0.02 mm, respectively. The wet carbonation of hornblende, $Ca(Mg, Fe, Al)_5(Al,Si)_8O_{22}(F,OH)_2$, generated calcite, $CaCO_3$, magnesite, $MgCO_3$, and siderite, $FeCO_3$, as crystalline carbonation by-products, coexisting with amorphous aluminum silicate hydroxide clay-like by-product [5]. Since all these by-products are categorized as minimally soluble in water, it is possible to rationalize that they precipitated and covered surfaces of the non-carbonated underlying rocks, acting as the protective barrier layer to inhibit and delay the progression of carbonation of rock during lengthy exposure. Similarly, diorite consisting of three crystalline phases, anorthite, biotite, and quartz, might prevent further carbonation. In fact, our previous study demonstrated that the $scCO_2$/water preferentially reacted with anorthite, $CaAl_2Si_2O_8$, rather than with biotite in diorite. In the other words, the susceptibility of anorthite to wet carbonation was considerably higher that that of biotite [5]. In fact, the wet carbonation of anorthite converted it into three amorphous carbonation reaction by-products, calcium carbonate, aluminum silicate hydroxide clay-like compound, and silica, $2CaAl_2Si_2O_8 + 2CO_3^{2-} + 4H^+ \rightarrow 2CaCO_3 + Al_4Si_{4-x}O_{12-2x}(OH)_4 + xSiO_2$, while some biotite remained

intact. A possible interpretation for the remaining of non-carbonated biotie was that the precipitation and coverage of biotite's surface by these water-insensitive by-products inhibited its further carbonation. More importantly, if these by-products are formed at the outermost surface site of carbonated diorite rock, they might be responsible for alleviating the secondary wet carbonation of entire diorite rock, so minimizing the carbonation depth.

To visualize such carbonation-inhibiting and-delaying performance by these water-insensitive by-products, we explored the alternation of microstructure along with the changes in elemental composition of carbonated diorite's surfaces by HR-SEM coupled with EDX. Figure 8 shows HR-SEM images of the non-carbonated and carbonated diorites' surfaces. The non-carbonated diorite represents the typical morphological and topographical features of surfaces of diorite rock; in contrast, carbonated diorite has a quite different surface texture, particularly, the development of scale-like microstructure, verifying that carbonation altered the diorite's surface. Unlike granite, no porous microstructures were created. To understand the chemistry of these scale-like compounds, which seemingly prevented the generation of a numerous pores and cavities at the outermost surface site, we inspected the atomic composition of both non-carbonated and carbonated diorite using EDX concomitant with HR-SEM (Figure 9). For non-carbonated diorite, EDX did not detect either the C or F element in a ~1.5 μm thick superficial layer. Its atomic composition was 58.4 % O, 0.6 % Mg, 13.5 % Al, 22.4 % Si, 2.1 % K, 2.6 % Ca, and 0.4 % Fe, attributed to either the anorthite or the biotite phase or both. In comparison, the EDX result from carbonated diorite showed three major changes in atomic concentration: First, two new elements, C and F, was incorporated into superficial layer; second was a conspicuous reduction in the amount of O, Al, and Si atoms; and, finally was an increase in the amount of four atoms, Mg, K, Ca, and Fe. In the first change, the detection of a substantial amount of F atom in the carbonated diorite's subsurface along with the detection of C related to carbonation can be interpreted as follows; since F atom arise from biotite, like the biotite in granite, the biotite present in a superficial layer of diorite was carbonated to leach HF. Correspondingly, the increase in concentration of the Mg, K, Ca, and Fe atoms reflected

the precipitation of the Mg-, Ca-, and Fe-carbonates and potassium aluminum silicate, $KAlSiO_4$, as the water-insensitive carbonation by-products of the anorthite and biotite phases. Hence, although some HF dissociated from the carbonated biotite, the coverage of underlying diorite rock by these water-insensitive scale-like by-products delayed and mitigated its carbonation and, hence, the carbonation depth of diorite was minimal.

Loss in Weight

One serious concern raised form the test results described above was the erosion of granite caused by the formation of water-sensitive by-products, which were related directly to a loss in weight of rock. Contrarily, if the water-insensitive by-products were formed at the outermost surface site of rock, its eroding-caused weight loss could be restrained. Thus, it is very important to know the magnitude of carbonation-caused erosion of granite; exceeding this magnitude might impair the integrity of a granite-based EGS reservoir.

Accordingly, we monitored the loss in weight of granite during the exposure to $scCO_2$/water at 200°C for up to 42 days. Although the exposure temperature was lower than that in our previous exposure temperature of 250°C, HR-SEM image of 200°C-carbonated granites' surfaces disclosed a porous microstructure due to its erosion (not shown). Four other rocks, albite, hornblende, diorite, and quartz, also were exposed to the same environmental condition as that of granite, and thereafter, their weight loss was measured (Figure 10).

For granite, a loss in its weight of 0.75 % promptly occurred during the first 7 days exposure; beyond that, it monotonously increased to 0.88 % at 42 days. The similar trend was observed for albite and hornblende; namely, the pronounced weight loss took place in the first 7 days, and then, its loss gradually rose from 0.29 % and 0.14 % at 7 days to 0.37 % and 0.17 % after 42 days for albite and hornblende, respectively. In contrast, two rocks, diorite and quartz, displayed a very low weight loss, reflecting a less than 0.1 % after 42 days.

Nevertheless, among these rocks, granite exhibited the highest eroding-caused weight loss; its value after 42 days was ~2.4, ~5.2, ~9.8, and ~17.6 times greater than that of albite, hornblende, diortite, and quartz, respectively. Correspondingly, the ranking of magnitude of erosion was in a following order, granite > albite > hornblende > diorite > quartz. This information provided us with two importance rules for carbonated rocks: First, the rock with a lower rate of carbonation depth will have minimal loss in weight; second, the magnitude of erosion depended mainly on the kind of carbonate by-products. Thus, the carbonated granite and albite rocks containing Na- and K-carbonates exhibited a high magnitude of erosion than carbonated hornblende and diorite rocks containing Ca-, Mg-, and Fe-carbonates.

Conclusion

Granite rock consisting of three mineralogical components, anorthoclase-type albite and quartz as the major phases, and biotite mica as the minor one was exposed for up to 104 hours to $scCO_2$/water at 250°C under 13.78- and 17.23-MPs pressure. The susceptibility of biotite to reactions with ionic carbonic acid as wet carbonation reactant was higher than that of anorthoclase-type albite, while quartz had no significant chemical affinity with it. The reactions between anorthoclase-type albite and carbonic acid yielded four amorphous reaction by-products, sodium carbonate, potassium carbonate, a kaolinite clay-like compound, and silicon dioxide. For biotite, all its wet carbonation by-products, except for HF, were crystalline compounds including potassium aluminum silicate, quartz, siderite, and magnesite. A serious concern about carbonated compounds was their solubility in water: Na- and K- carbonates derived from anorthoclase-type albite's carbonation displayed considerable high solubility compared with that of siderite ($FeCO_3$) and magnesite ($MgCO_3$). Based upon the non-susceptibility of pure kaolinite clay to wet carbonation, the kaolinite clay-like by-product from anorthoclase-type albite's carbonation might remain unaltered, even if $scCO_2$ exposure was extended.

Nevertheless, despite only 104 hours exposure at 250°C, the leaching of the water-soluble carbonation by-products, Na- and K-carbonates and HF, played an essential role

in eroding granite, thereby creating a porous microstructure containing numerous large voids. Correspondingly, the carbonation depth of granite was ~ 1.27 mm under such condition. In contrast, its depth of other minerals, in particular, for hornblende and diorite, was considerable lower, reflecting less than 0.1 mm.

The eroding-caused weight loss of granite was determined by exposing it to $scCO_2$/water at 200°C for up to 42 days. Erosion caused a striking weight loss of 0.75 % in the first 7 days exposure; beyond that, it gradually rose to 0.88 % after 42 days. This value at 42-day exposure was ~2.4, ~5.2, ~9.8, and ~17.6 times higher than that of albite, hornblende, diortite, and quartz, respectively, under the same condition. Thus, the major factor governing the extent of weight loss of carbonated rocks was the sensitivity of carbonation by-products to water, namely, the formation of Na- and K-carbonates and HF by-products that we categorized as highly water-soluble and -dissolvable compounds, promoted the extent of erosion. In contrast, the water-insensitive Ca-, Mg,- and Fe-carbonate, $KAlSiO_4$, SiO_2, and clay-like by-products resulted in little weight loss. The former by-products arose from the carbonation of granite and albite rocks. Although, the carbonation of diorite generated some HF, most of carbonation by-products of diorite and hornblende were water-insensitive ones.

Figure 11 summarizes the reaction by-products formed by wet carbonation of granite, albite, diorite, and hornblende rocks and their susceptibility to solubility in water. As evident, the wet carbonation of non-layer silicate-type minerals, such as anorthoclase-type albite, albite, and anorthite, led to the amorphous reaction products; contrarily, the layered silicate-type minerals like biotite and hornblende formed crystalline reaction by-products after their wet carbonation. The more important issue about the reaction by-products was their susceptibility in water. Because the generation of a large amount of water-soluble by-products entailed high erosion on the rocks, the carbonated granite and albite rocks where the major reaction by-products were water-sensitive compounds had a higher erosion rate than carbonated biotite and hornblende minerals whose major reaction by-products were a lower susceptibility in water.

Figure 12 compares the erosion-promoting mechanism of carbonated granite rock with the erosion–inhibiting mechanisms of diorite rock. The erosion of granite occurred in the following three steps: 1) Its reaction with ionic carbonic acid in aqueous media; 2) formation of water-sensitive carbonate by-products; and, 3) their dissolution and leaching along with a release of CO_2. In contrast, the wet carbonation reactions of diorite precipitated water-insensitive scale-like by-products as the major reaction products on the non-carbonated underlying rock's surface. Importantly, such scale by-products formed in a superficial layer of carbonated diorite served in providing a protective barrier layer, which inhibits or retards the carbonation-caused erosion of the underlying rock. Therefore, the carbonation depth and weigh loss was minimal in hornblende and diorite.

However, in this limited information, there is no evidence whether such eroding-caused alteration of granite continues with longer exposure time. The precipitation and coverage by substantial amounts of insoluble clay-like by-products and quartz as well as water-insensitive carbonated compounds on underlying granite surfaces might mitigate a further progression of this erosion. Furthermore, our experiments were conducted under static, no flow $scCO_2$/water condition. Thus, if the rock is tested under a stirring, dynamic $scCO_2$/water condition, the extent of erosion might differ because any by-products adhering poorly to the fresh underlying rock could be scoured and dislodged from the rock's surface by the flowing $scCO_2$/water.

References

1. D.W. Brown, "A Hot Dry Rock Geothermal Energy Concept Utilizing Supercritical CO_2 Instead Of Water," Proceedings, Twenty-fifth Workshop on geothermal reservoir engineering, Stanford University, January 2000, pp. 233-238.
2. K. Pruess, "The TOUGH Codes-A Family Of Simulation Tools For Multiphase Flow And Transport Processes In Permeable Media," Vadose Zone J., 3 (2004) 738-746.
3. K. Pruess, "Enhanced Geothermal Systems (EGS) Using CO_2 As Working Fluid-A Novel Approach For Generating Renewable Energy With Simultaneous Sequestration Of Carbon", Geothermic, 35 (2006) 351-367.
4. K. Pruess, "On Production Behavior Of Enhanced Geothermal Systems With CO_2 As Working Fluid," Energy Convers. Manage., 49 (2008) 1446-1454.
5. T. Sugama, L. Ecker, and T. Butcher, "Carbonation Of Rock Minerals By Supercritical Carbon Dioxide At 250°C," BNL-93722-2010-IR, June 2010.
6. T. Sugama, L. Ecker, S. Gill, T. Butcher, and D. Bour, "Carbonation Of Clay Minerals Exposed To $Scco_2$/Water At 200° And 250°C," BNL-94369-2010-IR, November 2010.
7. S.F. Hodgson, "As Long As You're There, Consider The Granite," GRC bulletin, 39 (2010) 32-33.
8. V.C. Farmer and J.D. Russell, "The Infra-Red Spectra Of Layer Silicates", Spectrochimica Acta, 20 (1964) 1149-1173.
9. T. Uchino, T. Sakka, K. Hotta, and M. Iwasaki, "Attenuated Total Reflectance Fourier-Transform Infrared Spectra Of A Hydrated Sodium Silicate Glass", J. Am. Ceram. Soc., 72 (1989) 2173-2175.
10. T. Uchino, T. Sakka, and M. Iwaski, "Interpretation Of Hydrated States Of Sodium Silicate Glasses By Infrared And Raman Analyis", J. Am. Ceram. Soc., 74 (1991) 306-313.
11. B.N. Roy, "Infrared Spectroscopy Of Lead And Alkaline-Earth Aluminosilicate Glasses", J. Am. Ceram. Soc., 73 (1990) 846-855.

12. Y. Soog, A.L. Goodman, J.R. McCarthy-Jones, and J.P. Baltrus, “Experimental And Simulation Studies On Mineral Tapping Of CO_2 With Brine”, Energy Conversion and Management, 45 (2004) 1845-1859.
13. A. Berg and S.A. Banwart, “Carbon Dioxide Mediated Dissolution Of Ca-Feldspar: Implications For Silicate Weathering”, Chem. Geology, 163 (2000) 25-42.
14. J.M. Matter and P.B. Kelemen, “Permanent Storage Of Carbon Dioxide In Geological Reservoirs By Mineral Carbonation”, Natural Geoscience, 2 (2009) 837-841.
15. H. Lin, T. Fujii, R. Takisawa, T. Takahashi, and T. Hashida, “Experimental Evaluation Of Interactions In Supercritical CO_2/Water/Rock Minerals System Under Geologic CO_2 Sequestration Conditions”, J. Materi. Sci. 43 (2008) 2307-2315.
16. R.C. Weast, Handbook of Chemistry and Physics, Forth-Ninth Edition, The Chemical Rubber Co., 1969.

Table 1. Comparison between the *d*-spacing peak area ratios of anorthoclase-type albite (Aa)- and biotito (B)- to- quartz (Q), and biotito (B)-to –anorthoclase-type albite (Aa) before and after exposure to $scCO_2$/water.

***d*-spacing peak area ratio**	**Before exposure**	**After exposure**
Aa, d_{002}/ Q, d_{101}	0.80	0.49
B, d_{001}/ Q, d_{101}	0.25	0.09
B, d_{001}/ Aa, d_{002}	0.31	0.18

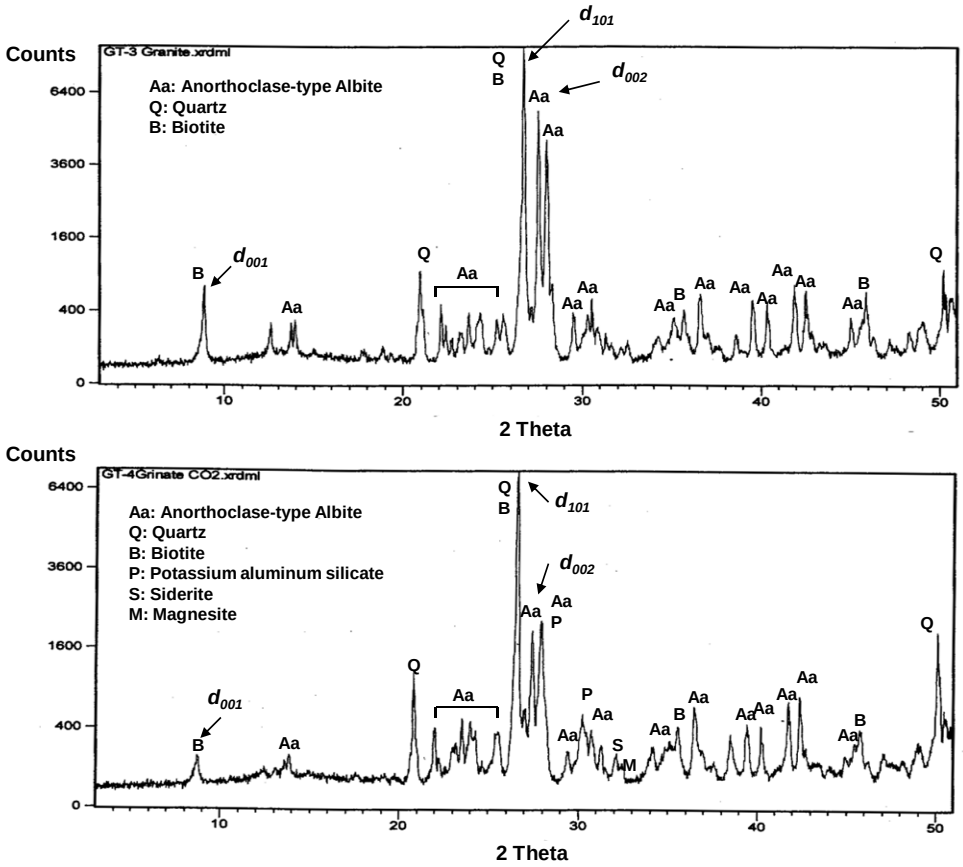

Figure 1. XRD patterns for granite mineral before (top) and after (bottom) exposure to $scCO_2$/water.

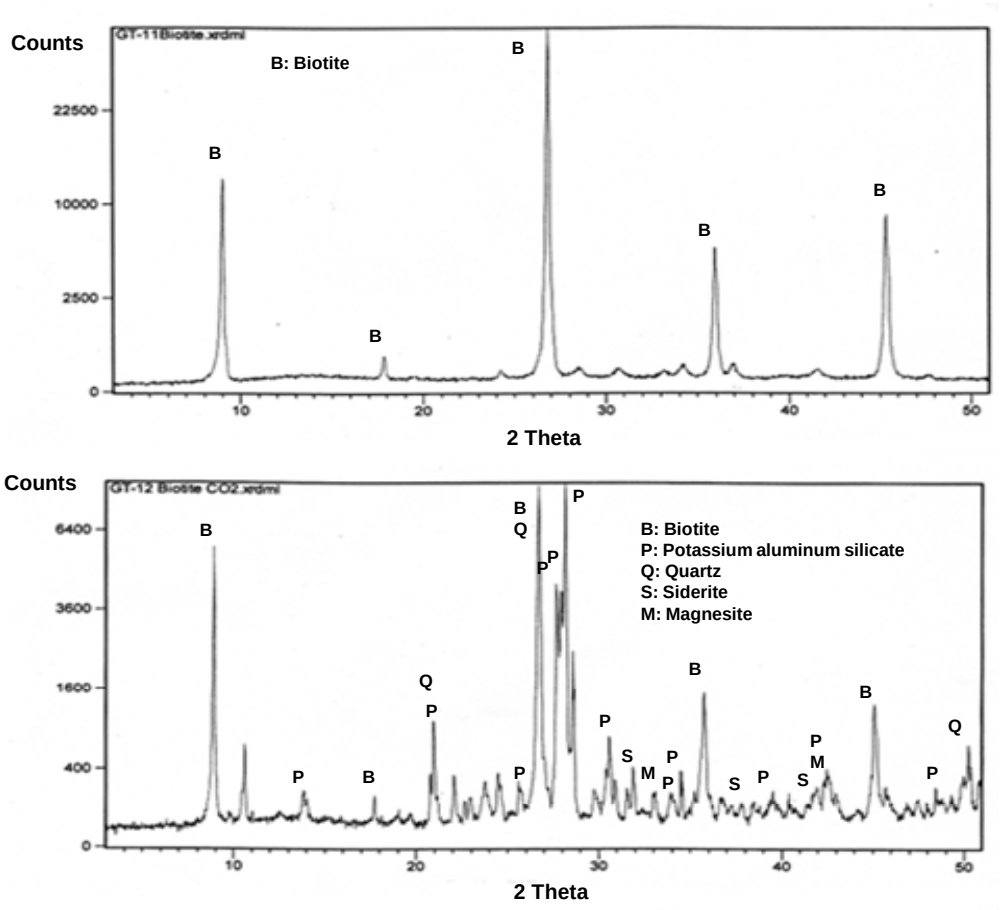

Figure 2. Comparison between XRD patterns of biotite before (top) and after (bottom) exposure to $scCO_2$/water at 250°C.

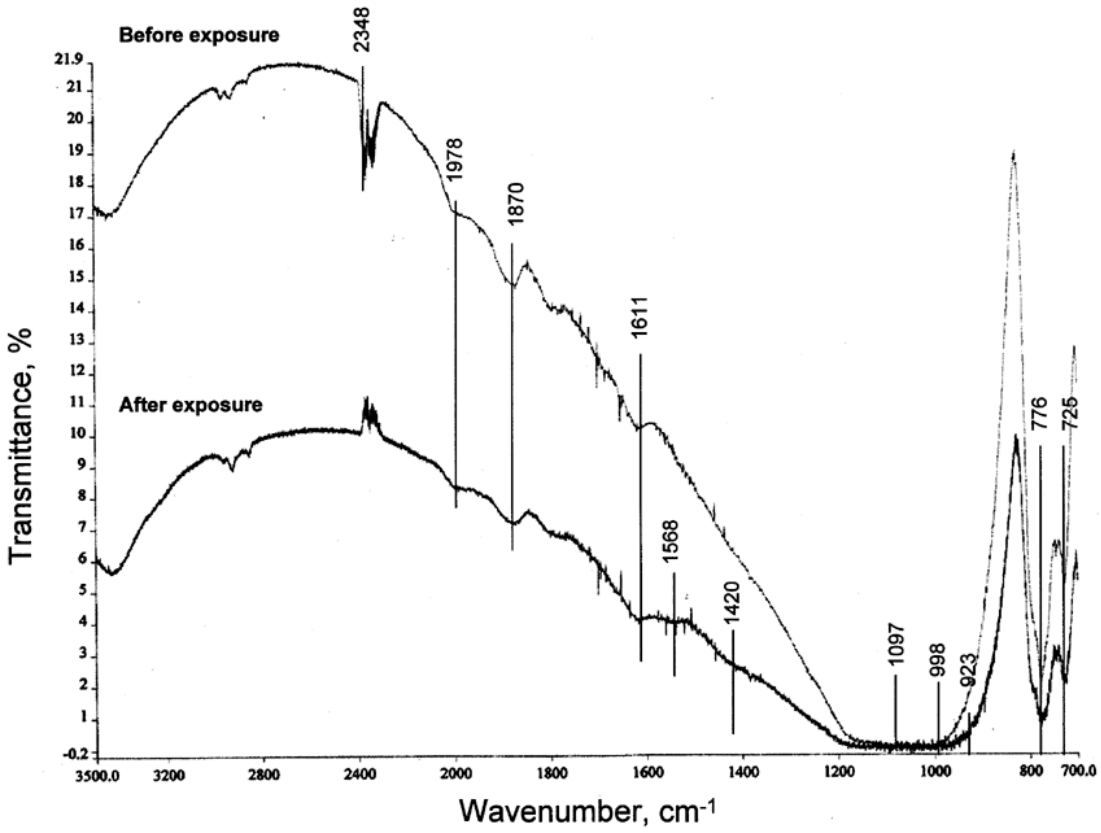

Figure 3. FT-IR spectra for unexposed and exposed granite to $scCO_2$/water.

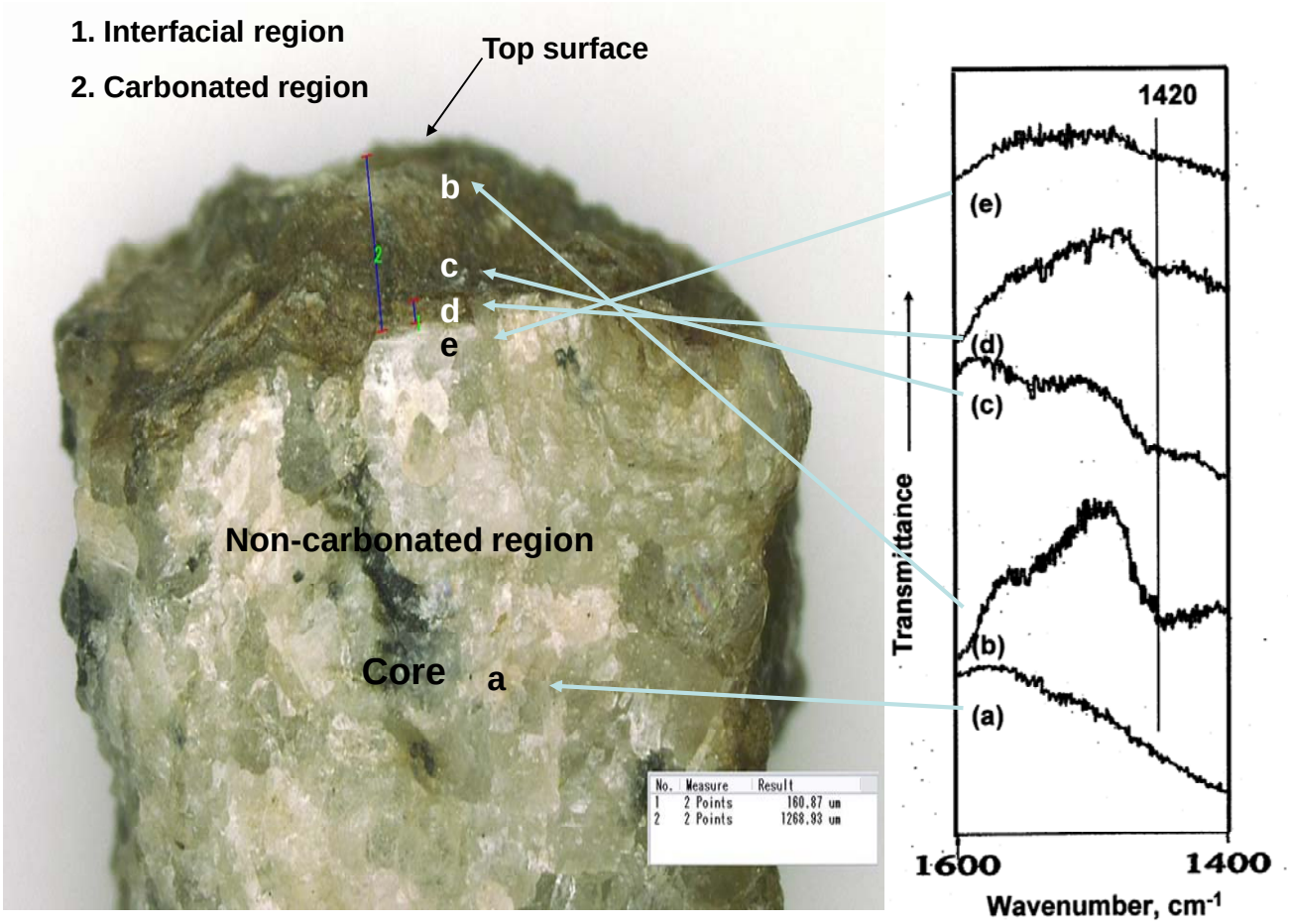

Figure 4. Carbonation depth profile from optical microscopy in conjunction with FT-IR inspection.

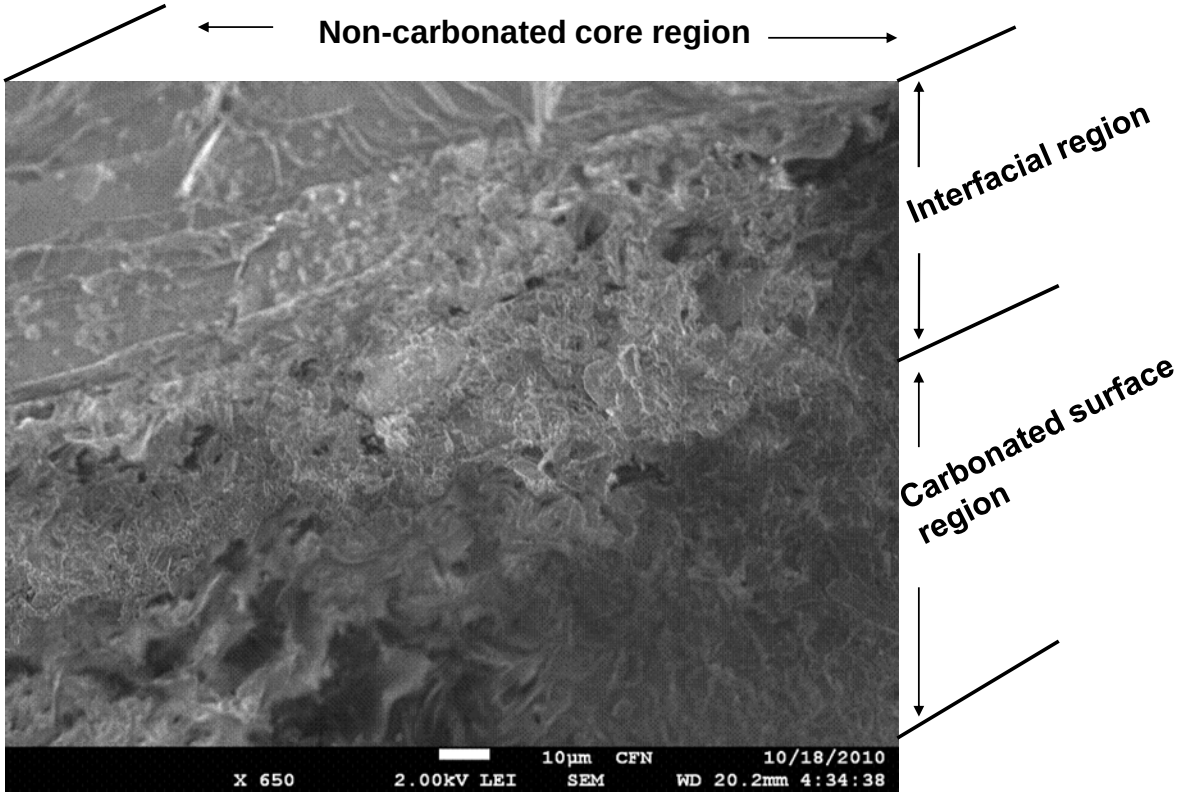

Figure 5. High resolution SEM image for the fractured surface of carbonated granite.

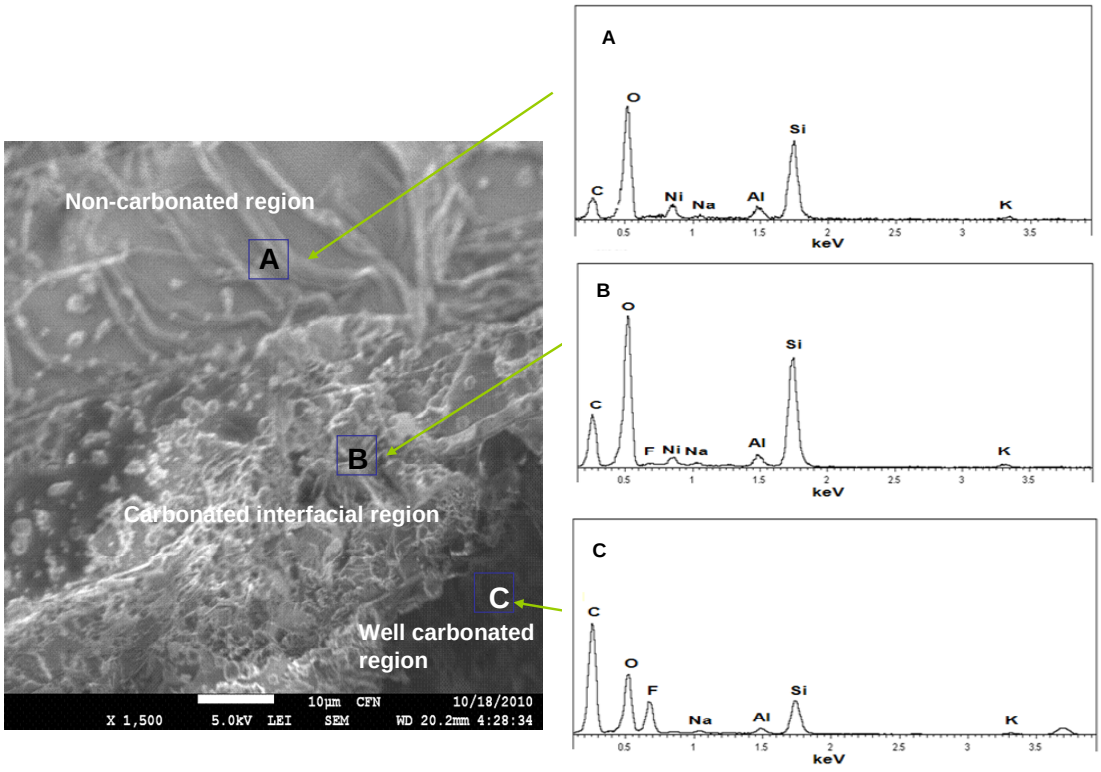

Figure 6. EDX elemental analysis at non-carbonated-, carbonated interfacial-, and well-carbonated-regions.

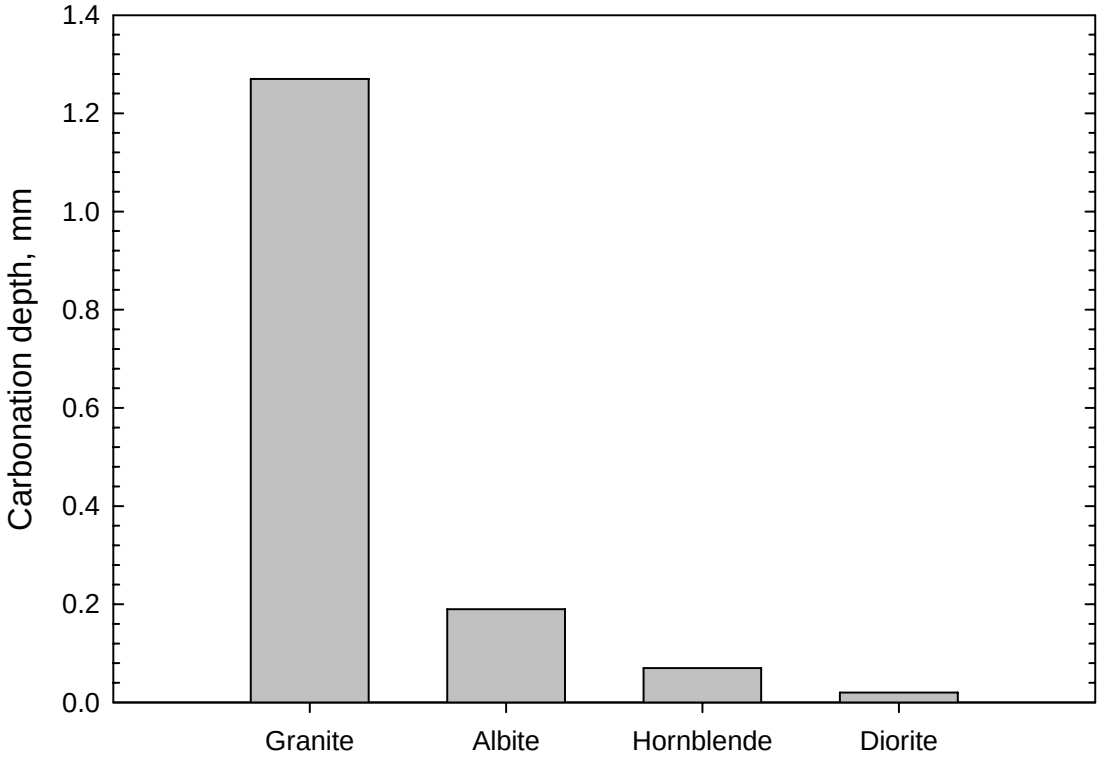

Figure 7. Carbonation depth of various rocks after exposure to $scCO_2$/water at 250°C for 104 hours.

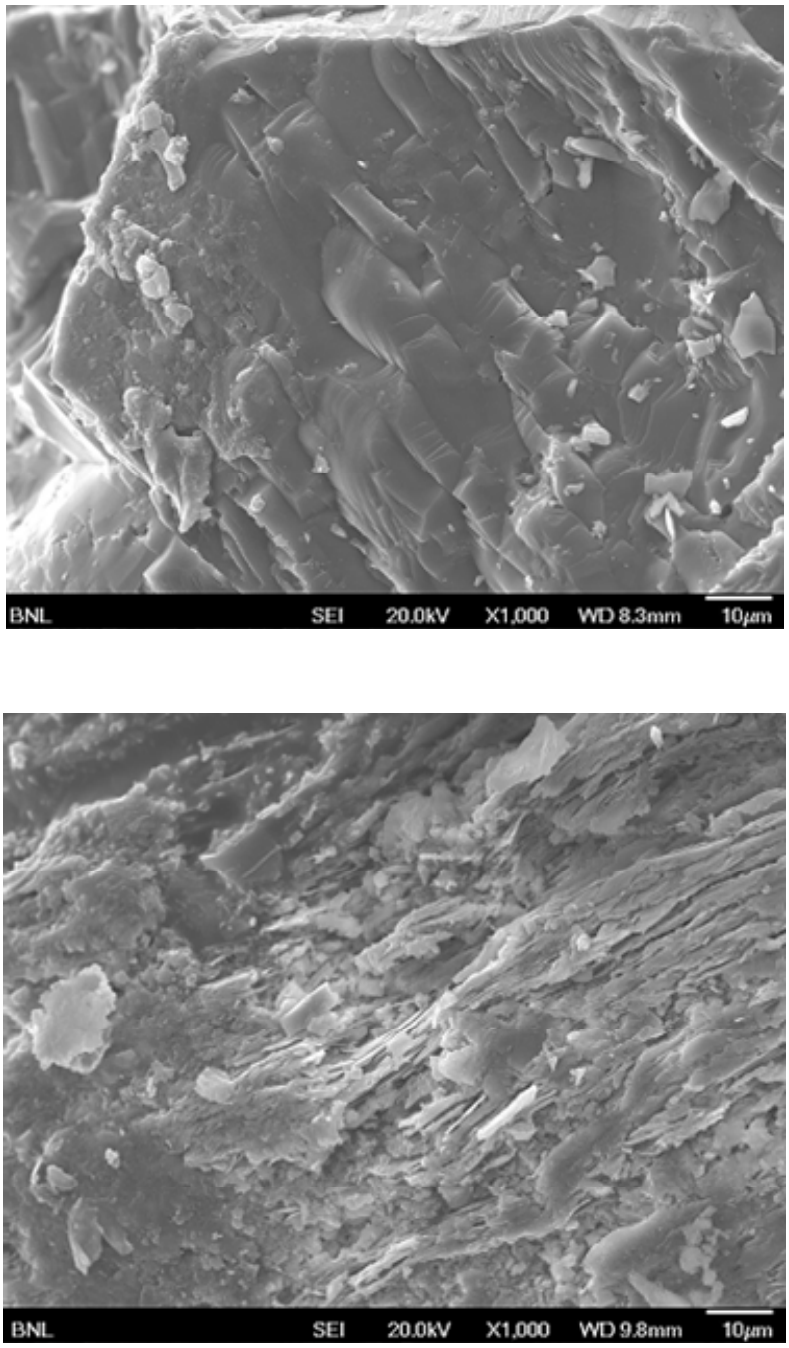

Figure 8. HR-SEM images of diorite rock surfaces before (top) and after (bottom) exposure to 250°C $scCO_2$/water.

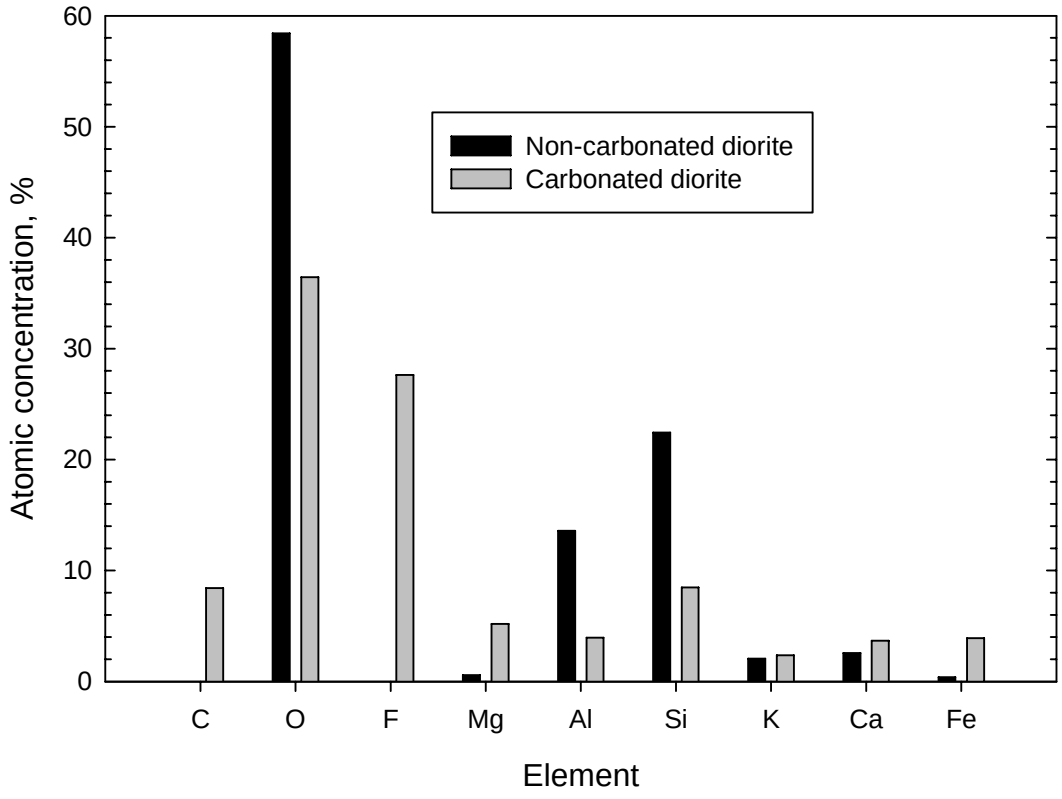

Figure 9. Comparison between atomic compositions of non-carbonated and carbonated diorite's surfaces by EDX.

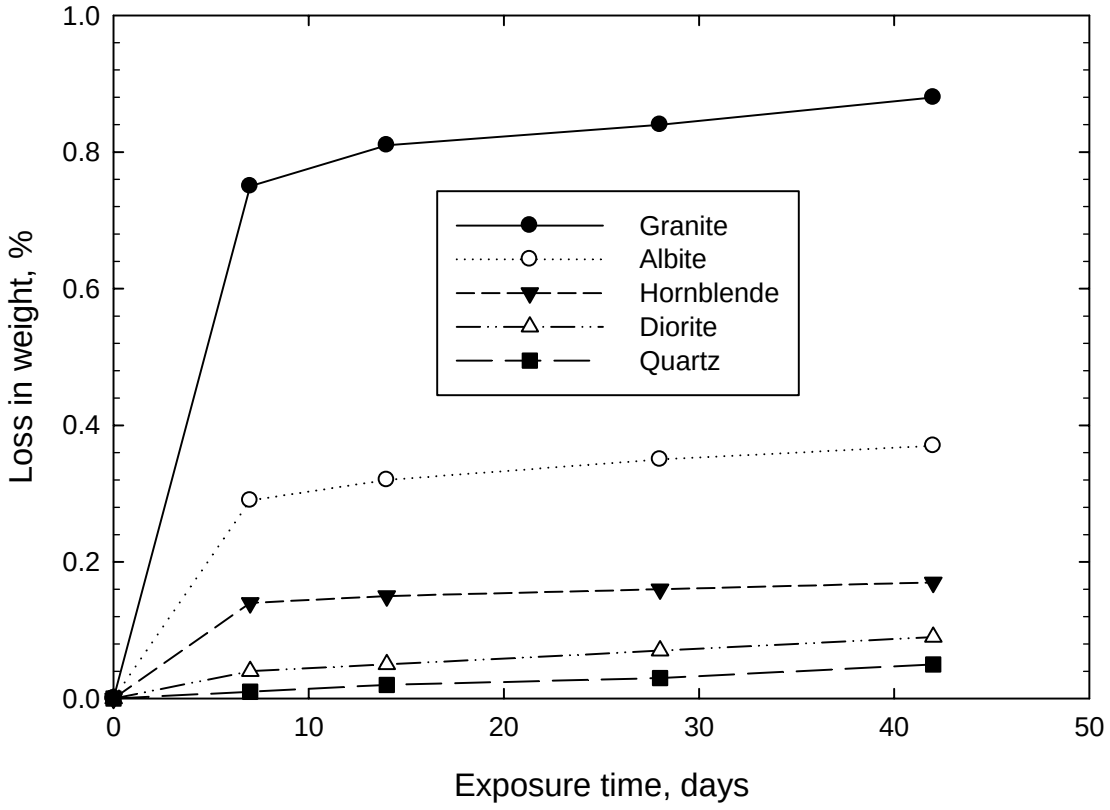

Figure 10. Changes in weight loss of various rocks as a function of $scCO_2$/water exposure time at 200°C.

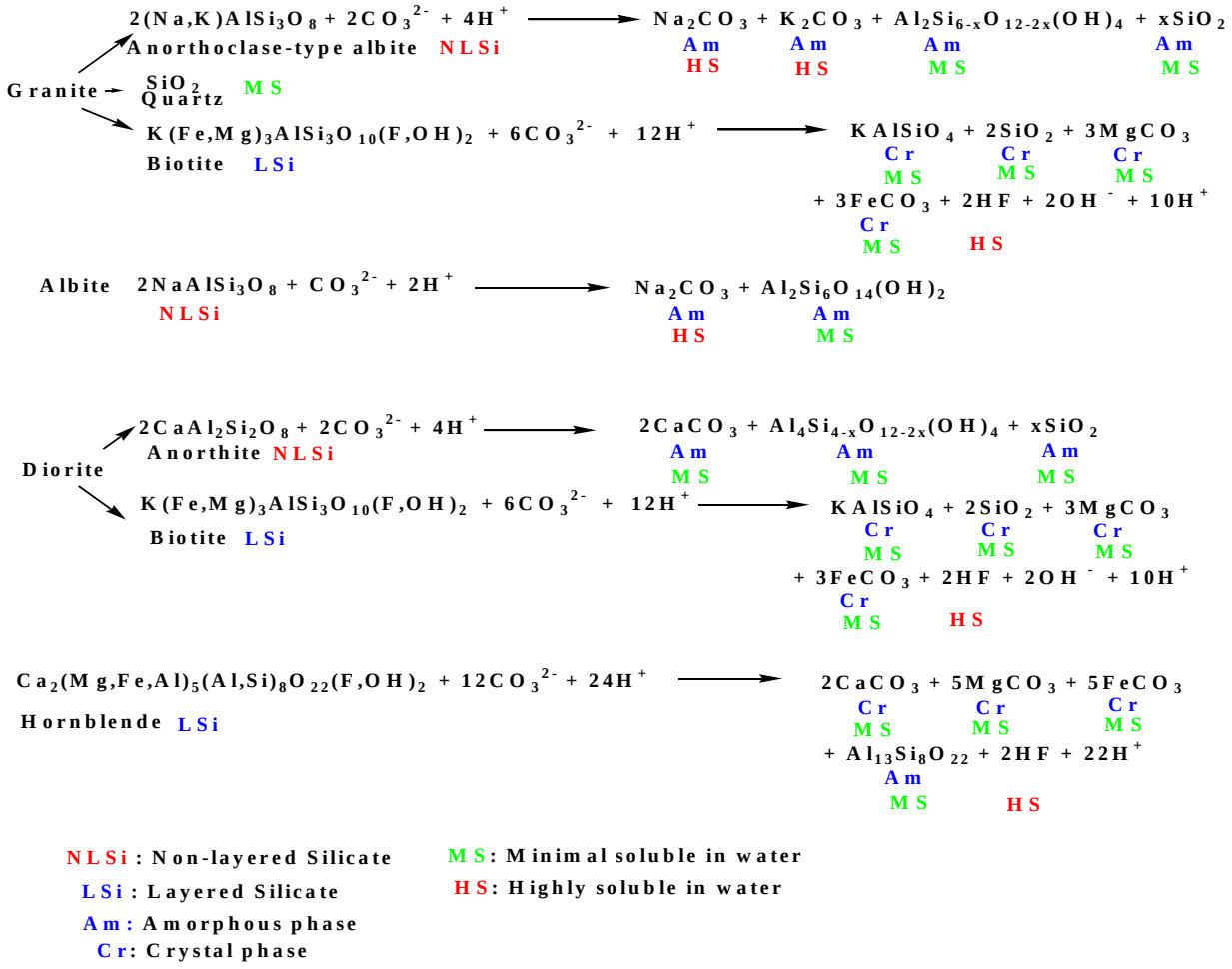

Figure 11. Summary of reaction products formed by wet carbonation of granite, albite, diorite, and hornblende rocks, and their susceptibility to solubility in water.

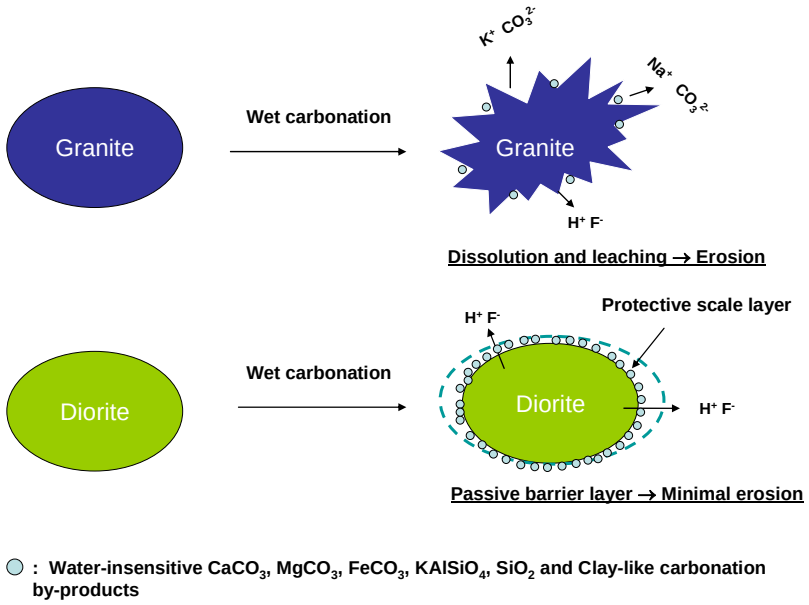

Figure 12. Erosion-promoting and –inhibiting mechanisms for granite and diorite rocks, respectively.